AGU
ADVANCING
EARTH AND
SPACE SCIENCES

Geophysical Research Letters®

Key Points:

- Rivers partition inorganic carbon between downstream transport and CO_2 emissions to the atmosphere
- Incorporating key hydrodynamic and biogeochemical processes, we identify the dimensionless numbers that govern the inorganic carbon partitioning
- Water hydrodynamics plays a critical role in the fate of the carbon that is out of equilibrium with the atmosphere

A Dimensionless Framework for the Partitioning of Fluvial Inorganic Carbon

Matteo B. Bertagni[1,2] [ORCID], **Pierre Regnier[3], Yanzi Yan[4]** [ORCID], **and Amilcare Porporato[2,5]**

[1]Department of Environment, Land and Infrastructure Engineering, Politecnico di Torino, Torino, Italy, [2]The High Meadows Environmental Institute, Princeton University, Princeton, NJ, USA, [3]Biogeochemistry and Modelling of the Earth System, Department Geoscience, Environment and Society, Université Libre de Bruxelles, Bruxelles, Belgium, [4]Department of Soil and Environment, Swedish University of Agricultural Sciences, Uppsala, Sweden, [5]Department of Civil and Environmental Engineering, Princeton University, Princeton, NJ, USA

Abstract Rivers are pivotal in the global carbon cycle, transporting terrestrial carbon to the ocean while emitting significant amount of CO_2 to the atmosphere. However, the partitioning of fluvial inorganic carbon (IC) between downstream transport and atmospheric evasion remains uncertain due to intricate hydrodynamic and biogeochemical processes. Inspired by Budyko's hydrological work, this study introduces a dimensionless framework to identify critical factors in fluvial IC partitioning: the IC fraction in equilibrium with the atmosphere and the ratio of advection to evasion timescales. River catchment analyses and modeling reveal that the equilibrium ratio determines the fraction of IC stably transported downstream. The hydrodynamic-driven timescale ratio determines the fate of out-of-equilibrium IC, with low-order streams favoring atmospheric evasion and higher-order streams promoting downstream transport. This framework provides a simple yet robust approach to predicting river carbon dynamics, with implications for land-to-ocean transport, fluvial emissions, and climate mitigation strategies such as enhanced weathering.

Plain Language Summary Rivers contain large amounts of dissolved inorganic carbon originating from the decomposition of organic matter and soil water fluxes. This carbon is partly transported downstream across the river network to the ocean and partly emitted as CO_2 to the atmosphere. Quantifying the partitioning between these fluxes is crucial for accurate carbon budgets from the local to the global scale, but the complex interplay of biogeophysical processes makes it challenging. Inspired by Budyko's seminal work in hydrology, we present a framework that determines the main chemical and physical processes governing the fluvial inorganic carbon partitioning. We identify two dimensionless numbers (or indexes) that can be defined with only a few parameters and provide quantitative and robust predictions on fluvial carbon fate. These numbers are linked to water turbulence and chemistry, and their values change across the river network.

1. Introduction

Although rivers cover only a small fraction of the Earth's surface (around 0.6%, Allen & Pavelsky, 2018), they play a critical role in the global carbon cycle, linking terrestrial, atmospheric, and marine systems (Aufdenkampe et al., 2011; Battin et al., 2023; Cole et al., 2007; Regnier et al., 2022). From headwater streams to estuaries, rivers and their associated channel-floodplain systems function as dynamic biogeochemical reactors where carbon is processed, buried, transported, or released to the atmosphere (Lauerwald et al., 2023; Wohl et al., 2017). Specifically, terrestrially derived organic carbon is transported across the river network to eventually reach the ocean, buried into sediments, or converted by biotic and abiotic processes into inorganic carbon (Hotchkiss et al., 2015). A possibly even larger amount of inorganic carbon enters rivers via water fluxes from riparian areas and groundwater systems (Battin et al., 2023; Duvert et al., 2018). As a result, rivers are often oversaturated in CO_2 and hotspots of CO_2 emissions to the atmosphere (Butman & Raymond, 2011; Raymond et al., 2013).

Quantifying riverine carbon fluxes on regional to global scales has thus become a focal point of recent research. This encompasses both emissions to the atmosphere (Lauerwald et al., 2023; Marx et al., 2017) and exports to the ocean, which are critical for assessing the land and ocean carbon sinks and, consequently, climate projections (Ciais et al., 2021; Lauerwald et al., 2020; Regnier et al., 2022). For instance, the evasion flux in the global fluvial network must be accounted for when determining the anthropogenic ocean carbon sink from observations (Jacobson et al., 2007; Regnier et al., 2022; Sarmiento & Sundquist, 1992). Global estimates of riverine carbon emissions have been revised upwards, from 0.2 to 0.5 Gt C/yr (Aufdenkampe et al., 2011; Cole et al., 2007) to
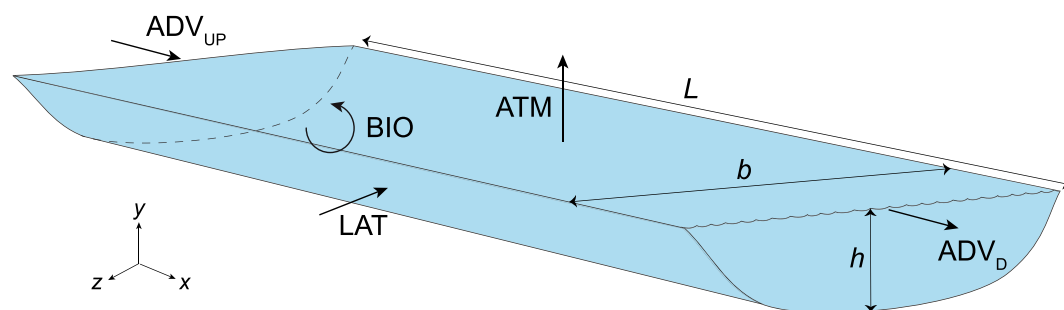
Figure 1. Sketch of the inorganic carbon fluxes in a river reach. ADV_{UP} and ADV_D are upstream and downstream advection, respectively; ATM is the evasion flux to the atmosphere; BIO is the net difference between organic matter decomposition and net primary production; LAT is the lateral input. In the text, total distributed inputs are defined as DIST = LAT + BIO.

approximately 2 Gt C/yr, reflecting extended observations and improved modeling techniques (Liu, Kuhn, et al., 2022; Raymond et al., 2013). Despite ongoing uncertainties, it is evident that these emissions are critical components of the global carbon cycle, comparable in magnitude to the anthropogenic terrestrial (2.8 Gt C/yr) and oceanic (3.1 Gt C/yr) carbon sinks (Friedlingstein et al., 2021).

Despite significant advances in estimating inorganic carbon (IC) fluxes in rivers, the detailed mechanisms controlling the IC partitioning between atmospheric evasion and downstream transport remain poorly understood (Vachon et al., 2021). Research often isolates one of the fluxes, neglecting that both are part of a single partitioning system controlled by chemical and physical processes. This challenge is similar to other partitioning issues in geophysics (Porporato, 2022) and, in particular, the hydrologic one studied by Budyko (1974): the partitioning of precipitation into evapotranspiration and runoff. Budyko (1974) first demonstrated that long-term rainfall partitioning can be understood through a dimensionless number (the dryness or aridity index) that encapsulates the climatic variables of a catchment. Since then, Budyko's framework has become a cornerstone in hydrology, providing a simplified yet robust method to understand the complex interactions between climate and the hydrological cycle without needing detailed, site-specific data.

Drawing inspiration from Budyko's seminal work, this paper proposes a dimensionless framework for partitioning fluvial IC. We aim to identify dimensionless numbers that govern this partitioning and elucidate the underlying hydrological and biogeochemical processes governing the overall dynamics. Initially, we develop the dimensionless framework based on dimensional considerations (Section 2). We then test the dimensionless framework using hydrodynamic and biogeochemical data for the reaches of the Susquehanna catchment, a major river in the Mid-Atlantic region of the United States (Section 3). Additionally, we present a physicochemical model for the inorganic carbon balance along a river reach to provide further theoretical insights into the role of the governing dimensionless groups (Section 4). We discuss our results, the work limitations, and the implications for climate mitigation strategies targeting inorganic carbon removal through alkalinity additions in the hydrological cycle, such as enhanced weathering (Section 5). Finally, we conclude with suggestions for future research (Section 6).

2. Inorganic Carbon Partitioning in a River Reach

2.1. Input and Output Fluxes

For a generic river reach (Figure 1), we focus on the long-term balance between inorganic carbon (IC) inputs and outputs, where IC includes dissolved inorganic carbon (DIC = CO_2 + HCO_3^- + CO_3^{2-}) and CO_2 gas. Inputs comprise advection from upstream (ADV_{UP}) and lateral fluxes from riparian soils (LAT). Internal IC production can occur due to the biotic decomposition of organic matter, which typically dominates over IC consumption by photosynthetic activity, indicating negative net ecosystem productivity (NEP<0, Battin et al., 2023; Butman et al., 2016). This net biotic IC source is referred to here as BIO. Dissolved inorganic carbon can also come from the dissolution of carbonate minerals in the river water, but this flux is usually negligible compared to lateral carbon inputs (Raymond & Hamilton, 2018). The total IC input (IN = ADV_{UP} + LAT + BIO) is partitioned into two output fluxes: downstream advection (ADV_D) and atmospheric evasion (ATM). Hence, the generic formula for the IC partitioning along a river reach can be written as

$$\text{IN} = \text{ATM} + \text{ADV}_D. \tag{1}$$

The mass balance Equation 1 is generally valid for any river reach, but, as we will show, the functional forms of its terms and the partitioning between evasion and downstream transport vary depending on river hydrodynamic and biogeochemical conditions. We stress that: (a) in the less common scenario that biotic processes act as an IC sink in the river water (i.e., photosynthetic activity dominating over organic matter decomposition), the term BIO can be moved from the input term (IN) on the left-hand side of Equation 1 to the right-hand side without loss of generality; (b) we neglect carbonate mineral precipitation due to the limited observational evidence of carbonate precipitation in rivers (Stumm & Morgan, 1996). (c) Riverine CO_2 emissions occur because the total IC input (IN) is typically much higher than the IC that the river can transport through advection under equilibrium conditions with the atmosphere (ADV_{eq}). In the following, the part of IC input that is out-of-equilibrium is indicated as $\Delta\text{IN} = \text{IN} - \text{ADV}_{eq}$.

2.2. Governing Dimensionless Groups

To identify the dimensionless groups controlling the IC partitioning (Equation 1), we perform a dimensional analysis (Barenblatt, 2003; Porporato, 2022) of the evasion flux ATM (Appendix A), which is a function of the river's hydrodynamic and biogeochemical features. Among the considered hydrodynamic features are: the water discharge (Q), velocity (U), width (b), depth (h), length (L), and CO_2 gas transfer velocity (k), which is related to the turbulence of river waters (Raymond et al., 2012, 2013). Governing biogeochemical features include the inorganic carbon entering from upstream $\left(\text{ADV}_{UP} = Q[\text{DIC}]_{UP}\right)$, the lateral IC input (LAT), the biotic production (BIO), and the IC that the river water can hold in equilibrium with the atmosphere. This can be defined as $\text{ADV}_{eq} = Q[\text{DIC}]_{eq}$, where the equilibrium DIC concentration is dictated by the air-water chemistry and, in particular, by the water alkalinity (refer to Text S1 in Supporting Information S1 for detailed aqueous carbonate chemistry).

Accounting for these hydrodynamic and biogeochemical features and using the Buckingham Π theorem (Barenblatt, 2003; Porporato, 2022), as detailed in Appendix A, results in the normalized atmospheric flux depending on three governing dimensionless groups

$$\frac{\text{ATM}}{\text{IN}} = f(\Pi_\tau, \Pi_{eq}, \Pi_{DIST}), \tag{2}$$

which are

$$\Pi_\tau = \frac{\tau_{adv}}{\tau_{ev}}, \Pi_{eq} = \frac{\text{ADV}_{eq}}{\text{IN}}, \Pi_{DIST} = \frac{\text{DIST}}{\text{IN}}. \tag{3}$$

The first group Π_τ is purely defined by the water hydrodynamics and represents the ratio between the time scale of advection ($\tau_{adv} = L/U$) and the time scale of CO_2 evasion ($\tau_{ev} = h/k$). This ratio is related to the gas footprint of a river, a common concept in river biogeochemistry (Demars et al., 2015; Rocher-Ros et al., 2023), and is reminiscent of a Damköhler number, the ratio of advection to reaction timescales, but with a physical (i.e., CO_2 evasion) rather than a chemical reaction. As we will later show, Π_τ is the most critical parameter in the IC partitioning. The other two dimensionless groups are related to the IC fluxes. The dimensionless group Π_{eq} defines the relative fraction of IC input in equilibrium with the atmosphere. Π_{DIST} represents the relative importance of distributed IC inputs, encompassing lateral fluxes and biotic production (DIST = LAT + BIO), as opposed to upstream advection ($1 - \Pi_{DIST}$). This dimensionless group is bounded by definition between 0 and 1.

3. River Catchment Analysis

Guided by the formulation above, we provide an in-depth analysis of IC partitioning and its governing dimensionless group for the reaches of a real-world catchment. Specifically, we examine the 1629 reaches of the Susquehanna River catchment, a major river in the Mid-Atlantic region of the United States, draining an area of around 71,000 km^2. Figure S1 in Supporting Information S1 shows the catchment map. Our analysis utilizes existing hydrodynamic and water chemistry data sets integrated with empirical laws and mass-balance modeling.
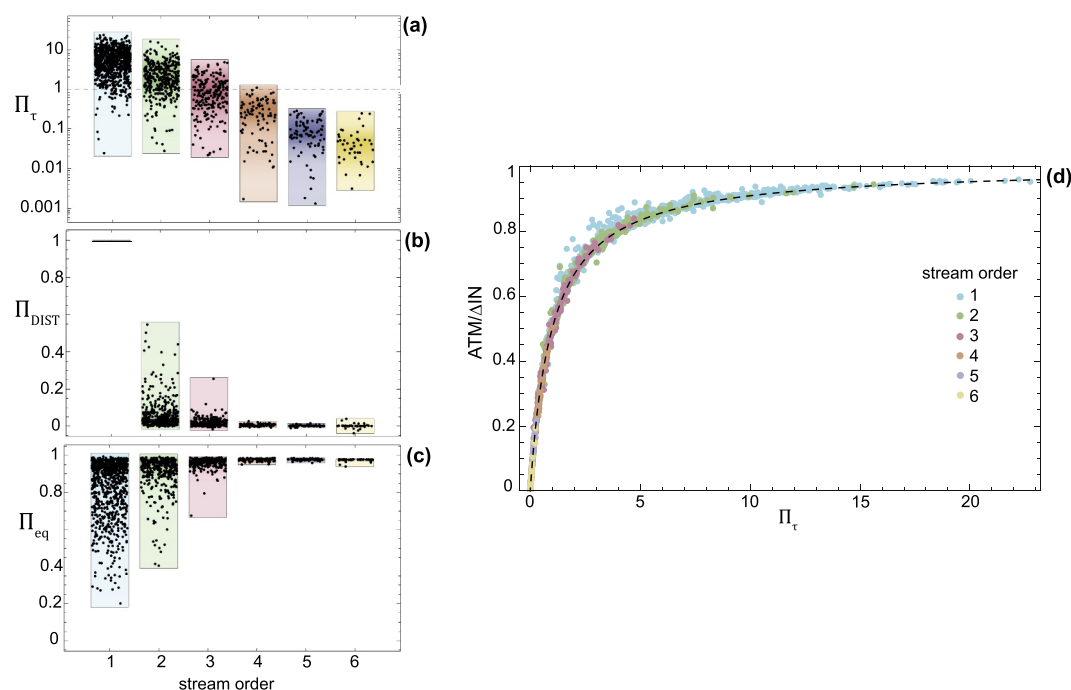
Figure 2. Analysis of the IC partitioning for the Susquehanna catchment. (a–c) Governing dimensionless groups for the river reaches (dots) grouped by stream order. (a) Timescale ratio. (b) Relative importance of distributed inputs. (c) Equilibrium ratio. (d) IC partitioning as a function of the timescale ratio. The partitioning is for the fraction of out-of-equilibrium carbon, $\Delta\text{IN} = \text{IN}(1 - \Pi_{eq}^{-1})$. The dashed line is $1/(1 + \Pi_{\tau}^{-1})$.

3.1. Hydrodynamic-Driven Transition in the Governing Timescale

To analyze the hydrodynamic features of the river reaches, we use data from GRADES, a global data set of daily discharge for 2.94 million reaches derived from the hydrographic data set MERIT-Hydro for 1980–2013 (Lin et al., 2019; Yamazaki et al., 2019; Yang et al., 2019). We obtained the average discharge value (Q), slope (S), and length (L) for each river reach. We then used empirical formulations from Raymond et al. (2012) to calculate the average velocity (U) and river width (b) as a function of the discharge, and the hydrodynamic-driven rate of CO_2 evasion (k) as a function of river velocity and slope. The typical flow depth (h) is derived as $h = Q/(U\,b)$.

These hydrodynamic features define the timescale ratio Π_{τ}. Figure 2a shows the results for the reaches of the Susquehanna catchment grouped by stream order. A clear trend emerges: lower stream orders (1 and 2) are characterized by an advection timescale that is longer than the evasion timescale ($\tau_{adv}/\tau_{ev} > 1$), indicating that CO_2 evasion is faster than downstream transport. Thus, most of the out-of-equilibrium IC entering these streams is expected to evade into the atmosphere before reaching the downstream reaches due to the elevated water turbulence that favors CO_2 degassing, as noted in previous studies (Horgby et al., 2019; Marx et al., 2017; Rocher-Ros et al., 2019). In contrast, higher stream orders (>4) exhibit an advection timescale shorter than the evasion timescale ($\tau_{adv}/\tau_{ev} < 1$), indicating predominant downstream transport of inorganic carbon.

3.2. Carbon Fluxes and Partitioning

To estimate carbon fluxes, we integrate water chemistry data with hydrodynamic data and mass balance modeling. We obtained yearly averaged aqueous CO_2 concentrations for each river reach from the global data set by Liu (2021). This data set comprises model outputs obtained with data-driven machine learning (Liu, Kuhn, et al., 2022). The concentrations in the Susquehanna catchment indicate CO_2 oversaturation between 2 and 6 times equilibrium values (Figure S2 in Supporting Information S1). We also used alkalinity values from the GLObal RIver Chemistry database (GLORICH, Hartmann et al., 2019). However, GLORICH covers only about 10% of the Susquehanna catchment's reaches (Hartmann et al., 2014), so we filled gaps using a mass balance approach along the river network (see Text S2.1 in Supporting Information S1). Combining alkalinity and

aqueous CO_2 concentration, the aqueous carbonate system of each reach is fully defined via water chemistry equations (Text S1.1 in Supporting Information S1).

Using the water hydrodynamical and chemical conditions, we can estimate the various IC fluxes. For each river reach, upstream advection (ADV_{UP}) is calculated as $Q[DIC]$, besides for the reaches of stream order 1, for which there is no upstream advection. For downstream advection, we assume that the water alkalinity is preserved (hence the bicarbonates, see Text S1.2 in Supporting Information S1), but that the CO_2 concentration is defined by the downstream reach $([CO_2]_D)$. Thus, downstream advection is calculated as $Q([DIC] - [CO_2] + [CO_2]_D)$. For the last stream (order 6) draining in the ocean, downstream advection is calculated as $Q[DIC]$. The atmospheric flux is modeled using a first-order closure to the degree of water oversaturation in CO_2, $ATM = k\,b\,L\left(\overline{[CO_2]} - [CO_2]_{eq}\right)$, where $\overline{[CO_2]} = ([CO_2] + [CO_2]_D)/2$ is an average CO_2 concentration between the considered reach and its downstream-connected component. Distributed inputs, accounting for lateral and biotic fluxes, result from the closure of the mass balance (Equation 1), namely $DIST = ATM + ADV_D\text{-}ADV_{UP}$.

Figures 2b and 2c show the resulting dimensionless groups (Π_{DIST} and Π_{eq}) obtained from the IC flux estimates. The relative importance of distributed carbon inputs (Π_{DIST}) decreases with stream order, going from 1 for the first stream order toward zero values for the last stream orders (Figure 2b). This indicates that upstream advection inputs become relatively more important than distributed inputs from low- to high-order streams. The equilibrium ratio (Π_{eq}) is highly variable for low-order streams and approaches 1 for higher-order streams (Figure 2c), indicating a small fraction of out-of-equilibrium carbon. This is due to the relatively low CO_2 oversaturation in the Susquehanna catchment and the high water alkalinity (>1000 μeq/L for most reaches), which results in a higher concentration of stable aqueous carbonates (i.e., HCO_3^-) compared to out-of-equilibrium CO_2 (Figure S4 in Supporting Information S1). These results also imply that, in the high-order streams of the Susquehanna, the amount of carbon that can evade into the atmosphere is much smaller than that stably transported downstream.

Combining the dimensionless groups, we can evaluate how the IC partitioning of the Susquehanna catchment varies as a function of governing hydrodynamic and biogeochemical processes. In particular, Figure 2d shows, as a function of the timescale ratio, the partitioning for the IC fraction that is out of equilibrium with the atmosphere, $ATM/\Delta IN$, where $\Delta IN = IN(1 - \Pi_{eq})$. The distance between the points and unity defines the downstream transport, $ADV_D/\Delta IN$. Almost all points representing the reaches of the Susquehanna catchment are scattered around a single curve, $1/(1 + \Pi_\tau^{-1})$ (dashed line), defined by the modeling of the IC fluxes (see Text S2.2 in Supporting Information S1 for analytical details). For $\tau_{adv}/\tau_{ev} < 1$ (high stream orders), the fraction of out-of-equilibrium carbon that evades into the atmosphere is low, with most carbon transported downstream. For $\tau_{adv}/\tau_{ev} \gg 1$ (low stream orders), most out-of-equilibrium carbon evades into the atmosphere, keeping the water close to equilibrium conditions. The partitioning for the total IC input (ATM/IN) is presented in Figure S3 of the Supporting Information S1, highlighting a large scatter of the reaches with $\tau_{adv}/\tau_{ev} \gg 1$ due to the different values of the equilibrium ratio Π_{eq}. This is an aspect that is further explored theoretically in the following section.

4. Modeling Framework

The analysis in the previous section highlighted how the timescale ratio (Π_τ) governs the partitioning of out-of-equilibrium carbon. Here, we consider the streamwise, spatially explicit DIC balance to provide further theoretical insights into the partitioning of equilibrium and out-of-equilibrium fractions and the role of the different governing parameters.

4.1. Spatially Varying Streamwise DIC Balance

The steady-state one-dimensional (1D) mass balance for dissolved inorganic carbon (DIC) in a river reach can be written as

$$\begin{cases} Q\dfrac{d}{dx}[DIC] = -\text{atm}(x) + \text{lat} + \text{bio} \\ [DIC]_{x=0} = [DIC]_{UP} \end{cases}, \qquad (4)$$
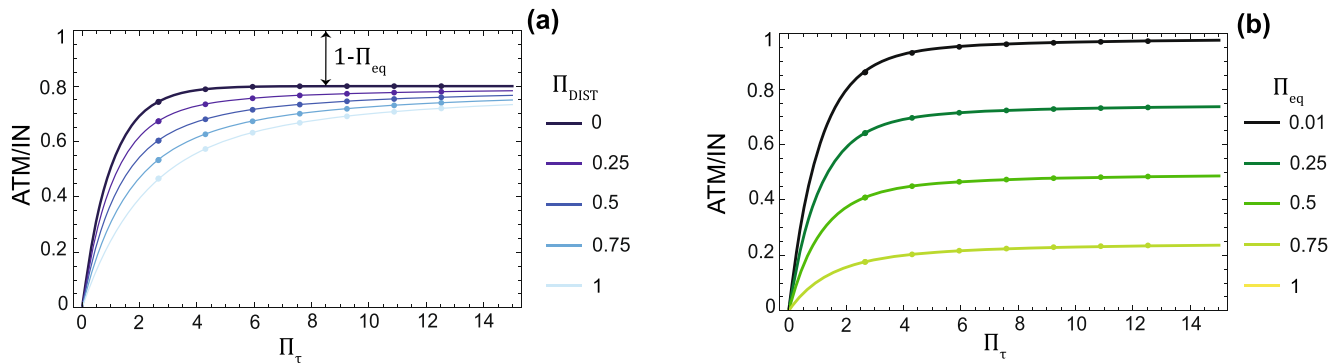
Figure 3. IC partitioning as a function of the timescale ratio (Π_τ) for different values of the governing dimensionless groups. (a) Influence of distributed inputs (Π_{DIST}), with Π_{eq} fixed to 0.2. (b) Influence of equilibrium ratio (Π_{eq}), with Π_{DIST} fixed to 0.2. The solid lines are from the analytical solution S12 (Supporting Information S1). Symbols are from the numerical solution of Equation 4.

where atm, lat, and bio are fluxes per unit length (dimension $M\ L^{-1}\ T^{-1}$), and x is the longitudinal coordinate. Equation 4 defines how the DIC varies along a river reach due to lateral and biotic inputs and carbon loss to the atmosphere. The evasion flux to the atmosphere is modeled using a first-order closure to the degree of water saturation in CO_2, atm(x) = $k\ b\ \Delta[CO_2]$. The water chemistry conditions define the relationship between DIC and CO_2 concentrations (Text S1.1 in Supporting Information S1). Ideally, Equation 4 can be solved for any x-dependence in river hydrodynamic and biogeochemical parameters. Here, we focus on a simple case where the river hydrodynamic features and lateral and biotic inputs are spatially uniform. A constant river discharge implies evaporation losses along the reach balance lateral water inputs. In these conditions, the Equation 4 also admits an approximated analytical solution with an explicit dependence on the governing dimensionless groups (Text S3 in Supporting Information S1).

4.2. Influence of Governing Groups

The 1D solution to Equation 4 can be integrated over the river reach length to evaluate the atmospheric flux and hence the IC partitioning. Here we present the partitioning results for the total IC input (ATM/IN) rather than its out-of-equilibrium fraction (ATM/ΔIN) to highlight the role of the equilibrium ratio. Figure 3 presents the partitioning as a function of the key controlling parameters: the timescale ratio (Π_τ), the relative importance of distributed inputs (Π_{DIST}), and the equilibrium ratio (Π_{eq}). Specifically, the solid lines are derived from the approximated analytical solution derived in Text S3 of the Supporting Information S1, and the symbols are obtained by numerically integrating the problem (Equation 4). The analytical and numerical solutions are indistinguishable. The distance of the curves to unity delineates the normalized downstream transport (ADV$_D$/IN).

For a given equilibrium ratio, the timescale ratio (Π_τ), namely the ratio between the timescales of advection and CO_2 evasion, is the most critical dimensionless group in the IC partitioning. When $\Pi_\tau \gg 1$, the advection time dramatically exceeds the evasion time, such that nearly all evasion has occurred and the river approaches equilibrium conditions, illustrated by the asymptote $1 - \Pi_{eq}$. By contrast, when $\Pi_\tau < 1$, there has not been enough time for the transported CO_2 to evade into the atmosphere, and a predominant downstream transport of inorganic carbon occurs. The different curves in Figure 3a suggest that distributed carbon inputs, Π_{DIST}, play only a second-order role in the partitioning shape, slightly varying its curvature. This curvature change could be more accentuated with less spatially uniform IC inputs.

The equilibrium ratio Π_{eq}, representing the fraction of carbon in equilibrium with the atmosphere, defines the asymptotic plateau of the partitioning curve (Figure 3b). In other words, Π_{eq} defines the relative portion of carbon input that can remain in the river water after equilibration with the atmosphere. In the limiting case where $\Pi_{eq} \rightarrow$ 1, all of the carbon entering the river can remain in the water, and there is no net CO_2 evasion (ATM$\rightarrow$0). Conversely, as $\Pi_{eq} \rightarrow 0$, virtually all carbon entering the river will tend to evade into the atmosphere. Notably, in the case of negligible distributed inputs ($\Pi_{DIST} \approx 0$), the partitioning curves can be vertically scaled with the asymptotic plateau ($1 - \Pi_{eq}$) to obtain a single curve for the partitioning of the out-of-equilibrium carbon (ATM/

ΔIN), as performed for the Susquehanna example (Figure 2d). In other words, the fate of the out-of-equilibrium carbon is only impacted by the timescale ratio and not by the equilibrium conditions.

5. Discussion

The dimensionless framework presented here offers a means to assess the relative significance of fluvial IC fluxes in the land-to-ocean transport, an essential yet poorly quantified aspect of the global carbon cycle (Regnier et al., 2022). Our findings highlight two governing dimensionless groups for quantitatively understanding IC fate in a river reach: Π_{eq}, which defines the relative fraction of carbon in equilibrium with the atmosphere, and Π_τ, which indicates the governing timescale for the fate of out-of-equilibrium carbon (i.e., evasion vs. downstream transport). Our model results and data analyses suggest that these two features can largely be decoupled (Figure 2d) due to the different governing processes. The partition between equilibrium and out-of-equilibrium IC is dictated by water chemistry conditions, while the partition between evasion and downstream transport of out-of-equilibrium carbon is influenced by water hydrodynamics and turbulence. Conversely, the relative importance of distributed inputs (Π_{DIST}) plays a second-order role in the partitioning.

In the reaches of the Susquehanna catchment, our analysis indicates that the fraction of out-of-equilibrium carbon evading into the atmosphere is significantly lower than the equilibrium carbon transported downstream, as evidenced by Π_{eq} values approaching 1 (Figure 2c). This is due to the high alkalinity levels and the low CO_2 oversaturation within these reaches, a condition that may vary considerably in other river systems. As a result, we find that the total inorganic carbon transported to the sea (744 Gg C/yr) is approximately three times greater than the carbon emitted as CO_2 (238 Gg C/yr) across the entire catchment. Additionally, we found that the timescale ratio varies from low-order streams dominated by evasion ($\Pi_\tau > 1$) to high-order streams dominated by downstream transport ($\Pi_\tau < 1$). This suggests that low-order streams characterized by high evasion rates will tend to equilibrate with the atmosphere relatively quickly, as supported by empirical studies (Horgby et al., 2019; Rocher-Ros et al., 2020). Extending our analyses for the Susquehanna catchment to the global scale could reveal if these stream-order controls are universally valid and if other climatic controls impact the values of the dimensionless numbers.

5.1. Limitations

Our results rely on average hydrodynamical or chemical values for the river reaches. Including more complex and spatially variable morphologies along the reach and more broadly across the river network could help quantify further hydrodynamic controls, especially in low-order streams characterized by nonlinear hydrodynamic features (e.g., hydraulic jumps). Furthermore, many hydrodynamic quantities, such as k and U, are parameterized by empirical equations that do not capture the full complexity of the physical processes involved. Although using different empirical formulas (e.g., Ulseth et al., 2019) could potentially affect the results quantitatively rather than qualitatively, issues related to uncertainty and unresolved physical processes would remain.

From a chemical perspective, integrating more spatially and temporally explicit data is challenging due to a generally limited coverage of observations. For example, only Rocher-Ros et al. (2019) have provided almost simultaneous, longitudinal measurements of CO_2 concentration over the reaches of a catchment. Global observation data sets are usually collections of single-point measurements, often scattered or unevenly distributed in time. This issue is even more pronounced for spatially distributed inorganic carbon inputs from land and biotic processes within the river waters, whose estimates mostly rely on modeling assumptions due to the limited observational constraint (Duvert et al., 2018; Rocher-Ros et al., 2019; Yao et al., 2021). Whether future research will provide sufficient detail to test this and other theoretical frameworks on spatially and temporally explicit data remains uncertain. Nevertheless, our framework is critical in providing scaling laws that embed the governing physical and chemical processes necessary to understand and quantify the IC transport along the land-to-ocean aquatic continuum.

5.2. Implications for Enhanced Weathering

Enhanced weathering is a nature-based climate mitigation strategy that involves dissolving silicate rocks rich in alkaline elements such as calcium (Ca) or magnesium (Mg) to promote aqueous carbonate (mostly HCO_3^-) formation in natural waters (Calabrese et al., 2022; Hartmann et al., 2013; Taylor et al., 2016). The rocks are

usually applied to croplands, and the weathering products are then transported by the hydrologic cycle to surface waters and the ocean, mitigating ocean acidification and sequestering atmospheric CO_2 for geological timescales (Renforth & Henderson, 2017). A critical open question is how the enhanced weathering products interact with the fluvial carbonate system.

Our framework highlights the critical role of the equilibrium ratio (Π_{eq}), which is directly linked to the water alkalinity and defines the fraction of carbon that is stably transported downstream. For typical river water chemistry (pH>6), alkalinity additions (Alk*) due to rock dissolution lead to an increase in the equilibrium carbon (ADV_{eq}^*) and hence in the equilibrium ratio, $\Pi_{eq} = (ADV_{eq} + ADV_{eq}^*)/IN$, for the same IC input. Thus, alkalinity additions to river systems imply more inorganic carbon being stably transported downstream and less CO_2 evasion. This supports the idea that direct river alkalinization might be a viable mitigation solution (Sterling et al., 2024).

The scenario is more complex when additional alkalinity comes from soils, potentially increasing IC flux from soil to river water (IN*). The impact on the equilibrium ratio depends on both changes in alkalinity and IC input, $\Pi_{eq} = (ADV_{eq} + ADV_{eq}^*)/(IN + IN^*)$, as influenced by the enhanced weathering application (i.e., load, rock type), hydrological connectivity, and soil and river chemistry (Bertagni & Porporato, 2022). Hence, specific scenarios must be developed for accurate assessments of the EW impact on fluvial carbon evasion.

6. Outlook

While this work focuses on inorganic carbon, the rationale and methods of this framework can be adapted to other inorganic or organic compounds transported and transformed in river systems. For instance, the partitioning of organic carbon between downstream transport and biotic conversion to inorganic compounds is governed by a Damköhler number analogous to the dimensionless group Π_τ (Liu, Maavara, et al., 2022). Other nutrients or pollutants may have additional governing dimensionless groups, as for the inorganic carbon case, suggesting that integrating such a framework could advance the development of catchment hydro-biogeochemical theories (Li et al., 2021). Future work could also extend the present framework to the continental and global scales, providing spatial patterns across different catchments and insights into hydroclimatic controls on the dimensionless numbers and inorganic carbon dynamics. Finally, the framework could also be extended to other aquatic systems, such as estuaries, for which we anticipate significant variations in the two governing dimensionless groups along their salinity gradients (Regnier et al., 2013; Vanderborght et al., 2002), and reservoirs, assessing their role in IC dynamics along fluvial networks.

Appendix A: Buckingham Π Theorem for Fluvial IC Partitioning

To identify the dimensionless groups controlling the IC partitioning (Equation 1), we perform a dimensional analysis (Barenblatt, 2003; Porporato, 2022) of the evasion flux ATM, which is a function of the river's hydrodynamic and biogeochemical features (listed in Section 2). The general function for the atmospheric flux can hence be written as

$$ATM = \psi\big(U, b, h, L, k, [DIC]_{UP}, [DIC]_{eq}, lat, NEP\big), \tag{A1}$$

where lat is the lateral IC input per unit length. The water discharge is not explicitly reported since it is a linear combination of the other quantities ($Q = b\, h\, U$). Temperature is also not explicitly reported, but its influence is embedded in the hydrodynamic, chemical, and biotic parameters (e.g., $[DIC]_{eq}$, k, NEP, etc.). The dimensions of the governing quantities are $L\, T^{-1}$ for U and k, L for b, h, and L, $M\, L^{-3}$ for DIC concentrations, $M\, L^{-1}\, T^{-1}$ for lat, and $M\, L^{-3}\, T^{-1}$ for NEP. The problem hence admits three dimensionally independent quantities in the dimensions LMT. However, given that longitudinal, transverse, and vertical processes have very different length scales $\big(L_x \gg L_z \gg L_y\big)$, we follow the approach of directional dimensional analysis and consider three-dimensionally independent length scales (Barenblatt, 2003; Porporato, 2022). The 5 independent quantities are hence defined as

$$[L] = L_x, \qquad [h] = L_y, \qquad [b] = L_z, \qquad [L/U] = T, \qquad [IN] = M/T, \tag{A2}$$

where the square brackets are used only in this equation to indicate dimensions following Maxwell's convention. To scale carbon fluxes, we use the total inorganic carbon input IN, which is a linear combination of the governing dimensional quantities, $\text{IN} = Q[\text{DIC}]_{\text{UP}} + L\,\text{lat} + L\,h\,b\,\text{NEP}$.

Given that there are 9 dimensional governing quantities and 5 independent quantities, using the Buckingham Π theorem (Barenblatt, 2003; Porporato, 2022) results in the normalized atmospheric flux depending on 4 governing dimensionless groups

$$\frac{\text{ATM}}{\text{IN}} = \psi'\left(\Pi_\tau, \Pi_{\text{BIO}}, \Pi_{\text{LAT}}, \Pi_{\text{eq}}\right), \tag{A3}$$

which are

$$\Pi_\tau = \frac{\tau_{\text{adv}}}{\tau_{\text{ev}}}, \Pi_{\text{eq}} = \frac{\text{ADV}_{eq}}{\text{IN}}, \Pi_{\text{LAT}} = \frac{\text{LAT}}{\text{IN}}, \Pi_{\text{BIO}} = \frac{\text{BIO}}{\text{IN}}. \tag{A4}$$

The first group Π_τ is purely defined by the water hydrodynamics, while the others relate to the IC fluxes. Π_{LAT} and Π_{BIO} represent the relative importance of lateral (LAT) and biotic ($\text{BIO} = \text{NEP}\,L\,b\,h$) inputs, respectively. Since their sum defines the relative importance of distributed inputs, we combine them into a single dimensionless number, $\Pi_{\text{DIST}} = \Pi_{\text{LAT}} + \Pi_{\text{BIO}}$, but this can be easily separated if one is interested in discriminating DIC produced internally or coming from external sources (Hotchkiss et al., 2015).

Data Availability Statement

For the analyses of the Susquehanna catchment, data of discharge, slope, and length data can be downloaded from the global data set GRADES (Lin et al., 2019; Yang et al., 2019). Data for aqueous CO_2 concentrations are from Liu (2021). Alkalinity data are from the GLObal RIver Chemistry database, GLORICH (Hartmann et al., 2019). The numerical code used for the analytical and numerical analyses of the spatially explicit DIC model are available at (Bertagni, 2024).

References

Allen, G. H., & Pavelsky, T. M. (2018). Global extent of rivers and streams. *Science*, *361*(6402), 585–588. https://doi.org/10.1126/science.aat0636

Aufdenkampe, A. K., Mayorga, E., Raymond, P. A., Melack, J. M., Doney, S. C., Alin, S. R., et al. (2011). Riverine coupling of biogeochemical cycles between land, oceans, and atmosphere. *Frontiers in Ecology and the Environment*, *9*(1), 53–60. https://doi.org/10.1890/100014

Barenblatt, G. I. (2003). *Scaling*. Cambridge University Press. (OCLC: ocm51316389).

Battin, T. J., Lauerwald, R., Bernhardt, E. S., Bertuzzo, E., Gener, L. G., Hall, R. O., et al. (2023). River ecosystem metabolism and carbon biogeochemistry in a changing world. *Nature*, *613*(7944), 449–459. https://doi.org/10.1038/s41586-022-05500-8

Bertagni, M. B. (2024). Fluvial inorganic carbon partitioning [Software]. *Zenodo*. https://doi.org/10.5281/zenodo.13771783

Bertagni, M. B., & Porporato, A. (2022). The carbon-capture efficiency of natural water alkalinization: Implications for enhanced weathering. *Science of the Total Environment*, *838*, 156524. https://doi.org/10.1016/j.scitotenv.2022.156524

Budyko, M. I. M. I. (1974). Climate and life. Retrieved from https://cir.nii.ac.jp/crid/1130282268683318528

Butman, D., & Raymond, P. A. (2011). Significant efflux of carbon dioxide from streams and rivers in the United States. *Nature Geoscience*, *4*(12), 839–842. https://doi.org/10.1038/ngeo1294

Butman, D., Stackpoole, S., Stets, E., McDonald, C. P., Clow, D. W., & Striegl, R. G. (2016). Aquatic carbon cycling in the conterminous United States and implications for terrestrial carbon accounting. *Proceedings of the National Academy of Sciences of the United States of America*, *113*(1), 58–63. https://doi.org/10.1073/pnas.1512651112

Calabrese, S., Wild, B., Bertagni, M. B., Bourg, I. C., White, C., Aburto, F., et al. (2022). Nano- to global-scale uncertainties in terrestrial enhanced weathering. *Environmental Science & Technology*, *56*(22), 15261–15272. https://doi.org/10.1021/acs.est.2c03163

Ciais, P., Yao, Y., Gasser, T., Baccini, A., Wang, Y., Lauerwald, R., et al. (2021). Empirical estimates of regional carbon budgets imply reduced global soil heterotrophic respiration. *National Science Review*, *8*(2), nwaa145. https://doi.org/10.1093/nsr/nwaa145

Cole, J. J., Prairie, Y. T., Caraco, N. F., McDowell, W. H., Tranvik, L. J., Striegl, R. G., et al. (2007). Plumbing the global carbon cycle: Integrating inland waters into the terrestrial carbon budget. *Ecosystems*, *10*(1), 172–185. https://doi.org/10.1007/s10021-006-9013-8

Demars, B. O., Thompson, J., & Manson, J. R. (2015). Stream metabolism and the open diel oxygen method: Principles, practice, and perspectives. *Limnology and Oceanography: Methods*, *13*(7), 356–374. https://doi.org/10.1002/lom3.10030

Duvert, C., Butman, D. E., Marx, A., Ribolzi, O., & Hutley, L. B. (2018). CO_2 evasion along streams driven by groundwater inputs and geomorphic controls. *Nature Geoscience*, *11*(11), 813–818. https://doi.org/10.1038/s41561-018-0245-y

Friedlingstein, P., Jones, M. W., O'Sullivan, M., Andrew, R. M., Bakker, D. C. E., Hauck, J., et al. (2021). Global carbon budget 2021. *Earth System Science Data Discussions*, 1–191. https://doi.org/10.5194/essd-2021-386

Hartmann, J., Lauerwald, R., & Moosdorf, N. (2014). A brief overview of the GLObal RIver CHemistry database, GLORICH. *Procedia Earth and Planetary Science*, *10*, 23–27. https://doi.org/10.1016/j.proeps.2014.08.005

Hartmann, J., Lauerwald, R., & Moosdorf, N. (2019). Glorich—Global river chemistry database [Dataset]. *PANGAEA*. https://doi.org/10.1594/PANGAEA.902360

Hartmann, J., West, A. J., Renforth, P., Köhler, P., De La Rocha, C. L., Wolf-Gladrow, D. A., et al. (2013). Enhanced chemical weathering as a geoengineering strategy to reduce atmospheric carbon dioxide, supply nutrients, and mitigate ocean acidification: Enhanced weathering. *Reviews of Geophysics*, *51*(2), 113–149. https://doi.org/10.1002/rog.20004

Horgby, A., Segatto, P. L., Bertuzzo, E., Lauerwald, R., Lehner, B., Ulseth, A. J., et al. (2019). Unexpected large evasion fluxes of carbon dioxide from turbulent streams draining the world's mountains. *Nature Communications*, *10*(1), 4888. https://doi.org/10.1038/s41467-019-12905-z

Hotchkiss, E. R., Hall Jr, R. O., Sponseller, R. A., Butman, D., Klaminder, J., Laudon, H., et al. (2015). Sources of and processes controlling CO_2 emissions change with the size of streams and rivers. *Nature Geoscience*, *8*(9), 696–699. https://doi.org/10.1038/ngeo2507

Jacobson, A. R., Mikaloff Fletcher, S. E., Gruber, N., Sarmiento, J. L., & Gloor, M. (2007). A joint atmosphere-ocean inversion for surface fluxes of carbon dioxide: 1. Methods and global-scale fluxes. *Global Biogeochemical Cycles*, *21*(1). https://doi.org/10.1029/2005GB002556

Lauerwald, R., Allen, G. H., Deemer, B. R., Liu, S., Maavara, T., Raymond, P., et al. (2023). Inland water greenhouse gas budgets for RECCAP2: 2. Regionalization and homogenization of estimates. *Global Biogeochemical Cycles*, *37*(5), e2022GB007658. https://doi.org/10.1029/2022GB007658

Lauerwald, R., Regnier, P., Guenet, B., Friedlingstein, P., & Ciais, P. (2020). How simulations of the land carbon sink are biased by ignoring fluvial carbon transfers: A case study for the Amazon basin. *One Earth*, *3*(2), 226–236. https://doi.org/10.1016/j.oneear.2020.07.009

Li, L., Sullivan, P. L., Benettin, P., Cirpka, O. A., Bishop, K., Brantley, S. L., et al. (2021). Toward catchment hydro-biogeochemical theories. *WIREs Water*, *8*(1), e1495. https://doi.org/10.1002/wat2.1495

Lin, P., Pan, M., Beck, H. E., Yang, Y., Yamazaki, D., Frasson, R., et al. (2019). Global reconstruction of naturalized river flows at 2.94 million reaches. *Water Resources Research*, *55*(8), 6499–6516. https://doi.org/10.1029/2019WR025287

Liu, S. (2021). Monthly pCO_2, gas transfer velocity and CO_2 efflux rate in global streams and rivers (the grades river networks) [Dataset]. *Dryad*. https://doi.org/10.5061/dryad.d7wm37pz9

Liu, S., Kuhn, C., Amatulli, G., Aho, K., Butman, D. E., Allen, G. H., et al. (2022). The importance of hydrology in routing terrestrial carbon to the atmosphere via global streams and rivers. *Proceedings of the National Academy of Sciences of the United States of America*, *119*(11), e2106322119. https://doi.org/10.1073/pnas.2106322119

Liu, S., Maavara, T., Brinkerhoff, C. B., & Raymond, P. A. (2022). Global controls on DOC reaction versus export in watersheds: A Damköhler number analysis. *Global Biogeochemical Cycles*, *36*(4), e2021GB007278. https://doi.org/10.1029/2021gb007278

Marx, A., Dusek, J., Jankovec, J., Sanda, M., Vogel, T., van Geldern, R., et al. (2017). A review of CO_2 and associated carbon dynamics in headwater streams: A global perspective: Carbon dioxide in headwater streams. *Reviews of Geophysics*, *55*(2), 560–585. https://doi.org/10.1002/2016RG000547

Porporato, A. (2022). Hydrology without dimensions. *Hydrology and Earth System Sciences*, *26*(2), 355–374. https://doi.org/10.5194/hess-26-355-2022

Raymond, P. A., & Hamilton, S. K. (2018). Anthropogenic influences on riverine fluxes of dissolved inorganic carbon to the oceans. *Limnology and Oceanography Letters*, *3*(3), 143–155. https://doi.org/10.1002/lol2.10069

Raymond, P. A., Hartmann, J., Lauerwald, R., Sobek, S., McDonald, C., Hoover, M., et al. (2013). Global carbon dioxide emissions from inland waters. *Nature*, *503*(7476), 355–359. https://doi.org/10.1038/nature12760

Raymond, P. A., Zappa, C. J., Butman, D., Bott, T. L., Potter, J., Mulholland, P., et al. (2012). Scaling the gas transfer velocity and hydraulic geometry in streams and small rivers: Gas transfer velocity and hydraulic geometry. *Limnology and Oceanography: Fluids and Environments*, *2*(1), 41–53. https://doi.org/10.1215/21573689-1597669

Regnier, P., Friedlingstein, P., Ciais, P., Mackenzie, F. T., Gruber, N., Janssens, I. A., et al. (2013). Anthropogenic perturbation of the carbon fluxes from land to ocean. *Nature Geoscience*, *6*(8), 597–607. https://doi.org/10.1038/ngeo1830

Regnier, P., Resplandy, L., Najjar, R. G., & Ciais, P. (2022). The land-to-ocean loops of the global carbon cycle. *Nature*, *603*(7901), 401–410. https://doi.org/10.1038/s41586-021-04339-9

Renforth, P., & Henderson, G. (2017). Assessing ocean alkalinity for carbon sequestration. *Reviews of Geophysics*, *55*(3), 636–674. https://doi.org/10.1002/2016RG000533

Rocher-Ros, G., Sponseller, R. A., Bergström, A.-K., Myrstener, M., & Giesler, R. (2020). Stream metabolism controls diel patterns and evasion of CO_2 in Arctic streams. *Global Change Biology*, *26*(3), 1400–1413. https://doi.org/10.1111/gcb.14895

Rocher-Ros, G., Sponseller, R. A., Lidberg, W., Mörth, C., & Giesler, R. (2019). Landscape process domains drive patterns of CO_2 evasion from river networks. *Limnology and Oceanography Letters*, *4*(4), 87–95. https://doi.org/10.1002/lol2.10108

Rocher-Ros, G., Stanley, E. H., Loken, L. C., Casson, N. J., Raymond, P. A., Liu, S., et al. (2023). Global methane emissions from rivers and streams. *Nature*, *621*(7979), 530–535. https://doi.org/10.1038/s41586-023-06344-6

Sarmiento, J. L., & Sundquist, E. T. (1992). Revised budget for the oceanic uptake of anthropogenic carbon dioxide. *Nature*, *356*(6370), 589–593. https://doi.org/10.1038/356589a0

Sterling, S., Halfyard, E., Hart, K., Trueman, B., Grill, G., & Lehner, B. (2024). Addition of alkalinity to rivers: A new CO_2 removal strategy.

Stumm, W., & Morgan, J. J. (1996). *Aquatic chemistry: Chemical equilibria and rates in natural waters* (3rd ed. ed.). Wiley.

Taylor, L. L., Quirk, J., Thorley, R. M. S., Kharecha, P. A., Hansen, J., Ridgwell, A., et al. (2016). Enhanced weathering strategies for stabilizing climate and averting ocean acidification. *Nature Climate Change*, *6*(4), 402–406. https://doi.org/10.1038/nclimate2882

Ulseth, A. J., Hall, R. O., Boix Canadell, M., Madinger, H. L., Niayifar, A., & Battin, T. J. (2019). Distinct air–water gas exchange regimes in low- and high-energy streams. *Nature Geoscience*, *12*(4), 259–263. https://doi.org/10.1038/s41561-019-0324-8

Vachon, D., Sponseller, R. A., & Karlsson, J. (2021). Integrating carbon emission, accumulation and transport in inland waters to understand their role in the global carbon cycle. *Global Change Biology*, *27*(4), 719–727. https://doi.org/10.1111/gcb.15448

Vanderborght, J. P., Wollast, R., Loijens, M., & Regnier, P. (2002). Application of a transport-reaction model to the estimation of biogas fluxes in the Scheldt estuary. *Biogeochemistry*, *59*(1/2), 207–237. https://doi.org/10.1023/a:1015573131561

Wohl, E., Hall, R. O., Lininger, K. B., Sutfin, N. A., & Walters, D. M. (2017). Carbon dynamics of river corridors and the effects of human alterations. *Ecological Monographs*, *87*(3), 379–409. https://doi.org/10.1002/ecm.1261

Yamazaki, D., Ikeshima, D., Sosa, J., Bates, P. D., Allen, G. H., & Pavelsky, T. M. (2019). MERIT hydro: A high-resolution global hydrography map based on latest topography dataset. *Water Resources Research*, *55*(6), 5053–5073. https://doi.org/10.1029/2019WR024873

Yang, Y., Pan, M., Beck, H. E., Fisher, C. K., Beighley, R. E., Kao, S.-C., et al. (2019). Quest of calibration density and consistency in hydrologic modeling: Distributed parameter calibration against streamflow characteristics. *Water Resources Research*, *55*(9), 7784–7803. https://doi.org/10.1029/2018WR024178

Yao, Y., Tian, H., Pan, S., Najjar, R. G., Friedrichs, M. A. M., Bian, Z., et al. (2021). Riverine carbon cycling over the past century in the Mid-Atlantic region of the United States. *Journal of Geophysical Research: Biogeosciences*, *126*(5), e2020JG005968. https://doi.org/10.1029/2020JG005968